Title

Anisotropy-dependent macroscopic domain structure in wedged-permalloy/uniform-FeMn bilayers

Journal

Journal of Applied Physics, 87(9)

ISSN

0021-8979

Authors

Liu, Kai
Zhou, SM
Chien, CL
et al.

Publication Date

2000-05-01

DOI

10.1063/1.373245

Peer reviewed

Anisotropy-dependent macroscopic domain structure in wedged-permalloy/uniform-FeMn bilayers

Kai Liu,[a] S. M. Zhou, and C. L. Chien[b]
Department of Physics and Astronomy, The Johns Hopkins University, Baltimore, Maryland 21218

V. I. Nikitenko,[c] V. S. Gornakov,[c] A. J. Shapiro, and R. D. Shull
Metallurgy Division, National Institute of Standards and Technology, Gaithersburg, Maryland 20899

Macroscopic domain structures have been realized in wedged-permalloy (Py)/uniform-FeMn bilayers during magnetization reversal. When the exchange anisotropy is established perpendicular or parallel to the wedge direction, two macroscopic domains are observed. Separating these domains are a 180° wall in the perpendicular geometry and an intermediate band containing large density of stripe-type microdomains in the parallel geometry. While the exchange field remains practically the same in both geometries, the coercivity and squareness of the loop are much less in the parallel geometry. © *2000 American Institute of Physics.* [S0021-8979(00)59208-1]

Since its discovery in 1956 by Meiklejohn and Bean,[1] exchange coupling across a ferromagnetic (FM)/antiferromagnetic (AF) interface has been an intriguing phenomenon. Despite extensive research efforts on the subject[2–14] and the technological applications of exchange coupling in spin-valve field-sensing devices,[15] the understanding of exchange coupling remains unsatisfactory. The early model assuming rigid AF spin structures has serious discrepancies with experimental results, particularly with regard to the values of the exchange field H_E and the coercivity H_C.[1] Several recent models have featured both FM and AF domains and provided more realistic predictions.[3,4,8,11,13,16] However, direct observation of the AF domains in such systems has been intrinsically difficult and not yet realized to date, whereas the detail study of the FM domain wall (DW) formation and motion is hampered by the presence of a large number of domains during switching.[17]

Recently, we have demonstrated that simple macroscopic domain structures in wedged-Py ($Ni_{81}Fe_{19}$)/uniform-FeMn ($Fe_{50}Mn_{50}$) bilayers can be created due to the inverse dependence of the exchange field on the FM layer thickness.[12] We have shown that when the exchange anisotropy is introduced perpendicular to the wedge direction, magnetization switching involves only two macroscopic domains. Such a system can be used as a model system to probe the domain dynamics in exchange-coupled systems.

In this work, we compare the features of the magnetization reversal processes in wedged-Py/uniform-FeMn bilayer system with the exchange anisotropy induced either *perpendicular or parallel* to the wedge direction. Using an advanced magneto-optical indicator film (MOIF) technique,[9,11] we have confirmed the simple domain structure and have investigated the transition region between the two macroscopic domains.

Specimens of Py(20–300 Å wedge)/FeMn(300 Å)/Cu(300 Å)/Si have been fabricated using the process described earlier.[12] The Cu buffer layer promotes the face-centered-cubic (fcc) (111) growth of the AF FeMn. The dimensions of the samples are about 5 cm×2 cm, where the long dimension is the wedge direction. Unidirectional anisotropy, perpendicular or parallel to the wedge direction, has been introduced using a suitable field cooling procedure.[12] We will refer to these two geometries as perpendicular and parallel geometry. The wedge specimen was then cut into two halves along the wedge direction for magneto-optical Kerr effect (MOKE) and vibrating sample magnetometry (VSM) measurements, using samples along two parallel wedge directions separated by about 1 cm. The MOKE measurements were made on an uncut wedged specimen by directing the laser beam along the wedge direction, whereas the VSM measurements were made on small samples cut from the wedge specimen. During these measurements, the applied magnetic field was always along the cooling field direction, along which the unidirectional exchange coupling was set. Details of the experiments in the perpendicular geometry can be found in our previous publication.[12] Direct experimental study of the domain structure in the samples has been performed by using the MOIF technique.

Representative hysteresis loops measured by VSM in both perpendicular and parallel geometries are shown in Fig. 1. In each geometry, the amount of loop shift to the left of the origin and the width of the loop increase with decreasing Py thickness t_{Py}, i.e., both the exchange field H_E and the coercivity H_C increase with decreasing t_{Py}. Furthermore, with decreasing t_{Py}, the loop becomes increasingly more slanted, the degree of which can be characterized by ΔH, the width of switching of magnetization between $\pm\mathbf{M}$. Between the perpendicular and the parallel geometries, for the same Py thickness, the values of H_E are similar, but the value of H_C in the parallel geometry is smaller, and the value of ΔH is much larger, than the corresponding quantities in the perpendicular geometry. One also notes that the decreasing- and the increasing-field branches of the loop for thinner Py layers are not symmetrical. The asymmetry is barely appreciable in the perpendicular geometry but more apparent in the parallel geometry.

[a]Present address: Dept. of Physics, UCSD, La Jolla, California 92093-0319.
[b]Electronic mail: clc@pha.jhu.edu
[c]Also at: Institute of Solid State Physics, Russian Academy of Sciences, Chernogolovka, Russia 142432.

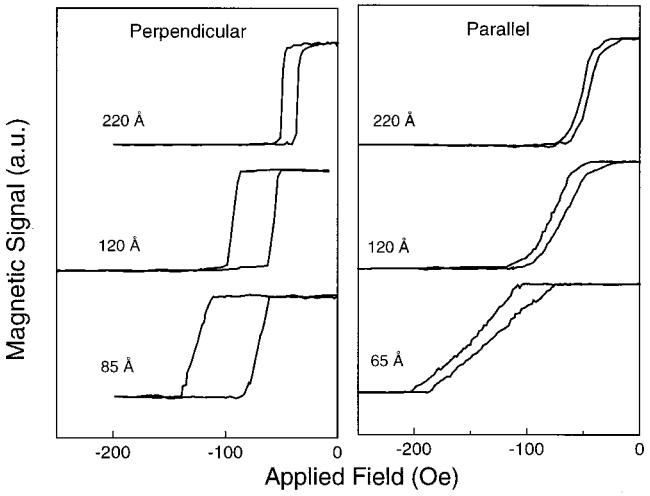

FIG. 1. Representative magnetic hysteresis loops of wedged-Py/uniform-FeMn bilayers at various Py thicknesses measured by VSM with exchange anisotropy perpendicular (left) and parallel (right) to the wedge direction.

Previously, we have demonstrated in the perpendicular geometry that the hysteresis loops measured by MOKE give the same values of H_E and H_C as those of the VSM measurements taken at the same corresponding locations along the wedge direction.[12] The fact that the results of the MOKE and VSM measurements are the same indicates the unique macroscopic domain structure in exchange-coupled wedged-Py/uniform-FeMn bilayer. Interestingly, the same agreement between MOKE and VSM has been observed in the parallel geometry, as shown in Fig. 2, where the measured values H_E and H_C determined by MOKE (solid symbols) and VSM (open symbols) are shown. For comparison, the corresponding values in the perpendicular geometry measured by MOKE are shown as crosses. It is clear that the value of H_E at the same t_{Py} is essentially the same in both geometries, whereas H_C is always larger in the perpendicular geometry. The $1/t_{\mathrm{Py}}$ dependence of the values of H_E and H_C in both

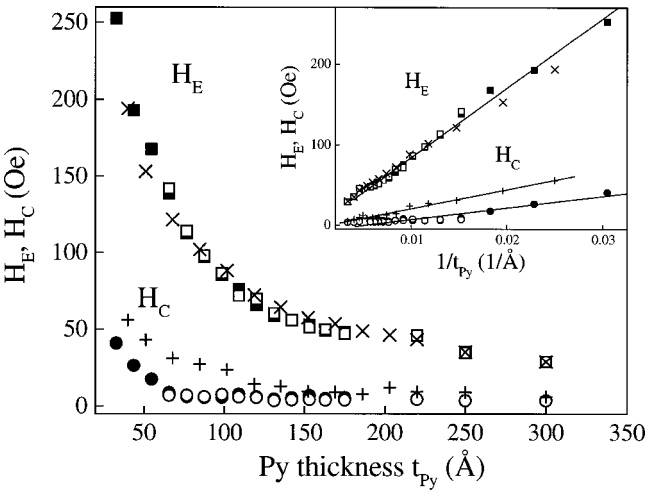

FIG. 2. Exchange field H_E and coercivity H_C of wedged-Py/uniform FeMn bilayers at various Py thicknesses t_{Py}. In the parallel geometry, the MOKE and VSM results are represented by solid and open symbols, respectively. In the perpendicular geometry, results are represented by crosses. The inset shows the inverse dependence of H_E and H_C on t_{Py}.

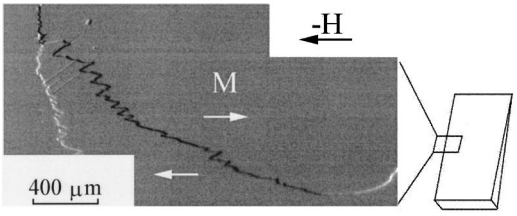

FIG. 3. MOIF image showing the 180° domain wall separating two macroscopic domains in the specimen where unidirectional anisotropy is perpendicular to the wedge direction. The imaging area is shown by the schematic. The magnetization direction is indicated by the white arrow.

geometries are shown in the inset of Fig. 2, in which one notes that the exchange fields in both geometries share the same slope, whereas the coercivities have different slopes in the two geometries.

The states with $+\mathbf{M}$ and $-\mathbf{M}$ are two single-domain states with magnetization pointing in the $+\mathbf{H}$ and the $-\mathbf{H}$ directions, respectively. In an exchange-coupled bilayer with a *uniform* FM layer, during the switching from $+\mathbf{M}$ and $-\mathbf{M}$, the entire FM layer breaks up into many domains with complicated patterns.[18] However, in the present *wedged*-Py/uniform FeMn system, where we have exploited the $1/t_{\mathrm{Py}}$ dependence of the exchange coupling, the transition between $\pm\mathbf{M}$ is restricted only to a small boundary region separating the two domains with $+\mathbf{M}$ and $-\mathbf{M}$.

In the perpendicular geometry, direct MOIF imaging of the domain structure have shown that the transition region is a 180° wall separating two macroscopic domains (Fig. 3). Different magnetostatic charges are imaged as bright and dark contrast, delineating domains and magnetization directions. The black-white contrast in the left part in Fig. 3 images the stray fields from left edge of the sample, as shown in the schematic. Magnetization reversal from the ground state begins at the two corners of the thick end of the wedge where the exchange anisotropy field (H_E) is minimal and the magnetostatic field (H_{MS}) is maximal. Reversal into the ground state begins from the central part of the thin end of wedge where H_E is maximal and H_{MS} is minimal. Further details of the domain formation and DW motion in this geometry are published elsewhere.[19]

In the specimen where the exchange anisotropy is established parallel to the wedge direction, two macroscopic domains are also observed. However the transition region between them is not a 180° DW. It is a band of intermediate region of considerable width containing large density of stripe-type microdomains. The evolution of magnetization reversal revealed by MOIF imaging in the parallel geometry is shown in Fig. 4. The imaged area is in the middle portion of the thick end of the wedge, as illustrated in the schematic in Fig. 4. Initially, the sample is fully magnetized, in a single-domain state with a positive field applied downwards (left schematic). Decreasing the field to -44 Oe, reversal domains begin to nucleate along the thick end of the sample, where H_E is minimal and H_{MS} is maximal. The original single domain in this part of the specimen has broken up into many small and narrow stripe-type domains, which are elongated perpendicular to the wedge direction. At -56 Oe, magnetization has practically switched at the thick end of the

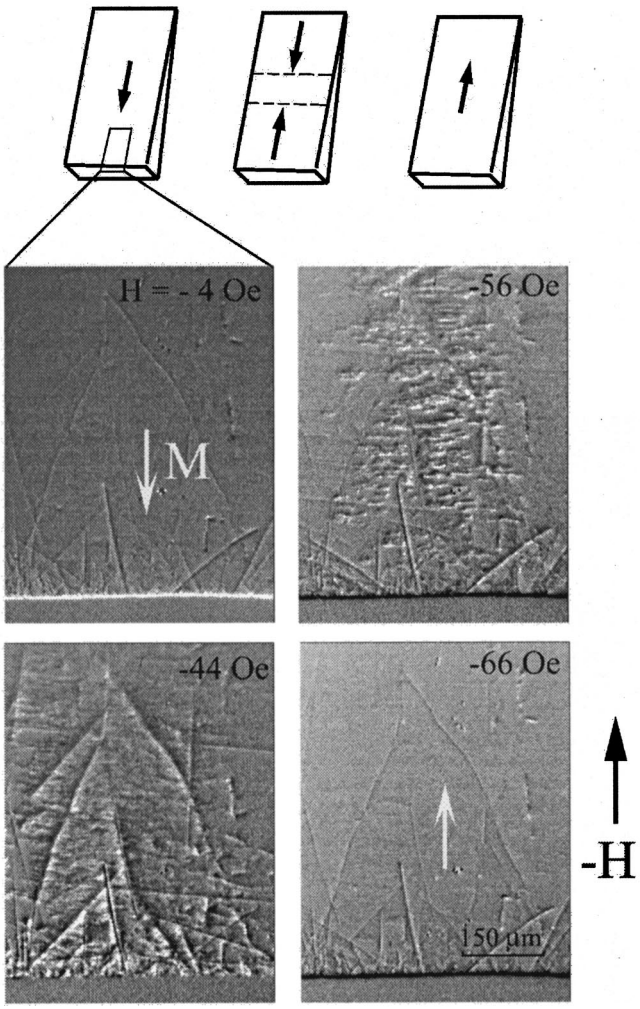

FIG. 4. MOIF images showing the evolution of magnetization reversal in the center of the thick end of the wedge. The schematics illustrate the imaging area and different stages of the magnetization reversal process.

wedge, indicated by the change of contrast from bright to dark at the sample edge. However, there are still a large number of stripe domains encompassed by the reversal domains. This band of microdomains gradually moves along the wedge direction (middle schematic). At a large negative field (-66 Oe), the band of microdomains is driven out of the thick end and moves towards the thin end. Finally at a sufficiently large negative field, the Py layer is completely magnetized upwards (right schematic).

The unique domain structures are also manifested in the shape of the hysteresis loops. In the perpendicular geometry, a 180° wall sweeps across the sample during the magnetization reversal process. Correspondingly, in a hysteresis loop, the width (ΔH) of the switching between $\pm\mathbf{M}$ represents the field increment needed to drive the wall across the sampling area. We have shown that the width of switching ΔH depends on both the Py layer thickness and the sample size.[12] The exchange coupling with anisotropy in the parallel geometry also affects the switching characteristics. In the parallel geometry, the intermediate band is much wider (hundreds of microns) than the 180° wall in the perpendicular case, switching from one single-domain state to the other is realized over much broader field range.

In summary, two macroscopic domains have been observed during magnetization switching in wedged-Py/uniform-FeMn bilayers, with the exchange anisotropy perpendicular or parallel to the wedge direction. But the macroscopic characteristics and kinetics of the magnetization reversal in these two types samples drastically differ. At the same Py thickness, the exchange field in the parallel geometry is the same as that in the perpendicular geometry, whereas the coercivity and the squareness are much less. Magnetization switching in the samples with the perpendicular geometry proceeds by a 180° DW motion. In the parallel geometry, remagnetization occurs due to the formation of a wide band of intermediate region with a large number of stripe-type microdomains and its motion along the wedge direction.

The different magnetization reversal patterns observed have two likely sources. First of all, it may be due to the different magnetostatic field distribution. In the perpendicular geometry, the magnetostatic field is determined by magnetic poles localized on the left and right sides of the wedge (refer to the schematic in Figs. 3 and 4). Whereas in the parallel geometry, it is determined by magnetic charges localized on thin and thick ends of the wedge, as well as over the whole wedge surface. Second, there may have been a change of an exchange spring penetration mechanism into the AF layer during the FM magnetization reversal. It can include a spin orientation phase transformation by spin flip or flop processes.[3,4,8,16] Each of these mechanisms could be responsible for the observed characteristics during magnetization reversal processes.

This work has been supported by NSF Grant Nos. DMR96-32526 and DMR97-32763.

[1] W. H. Meiklejohn and C. P. Bean, Phys. Rev. **102**, 1413 (1956); **105**, 904 (1957).
[2] C. Tang, N. Heiman, and K. Lee, J. Appl. Phys. **52**, 2471 (1981).
[3] D. Mauri, H. C. Siegman, P. S. Bagus, and E. Kay, J. Appl. Phys. **62**, 3047 (1987).
[4] A. P. Malozemoff, Phys. Rev. B **35**, 3679 (1987); **37**, 7673 (1988).
[5] J. Nogués, D. Lederman, T. J. Moran, and I. K. Schuller, Phys. Rev. Lett. **76**, 4624 (1996).
[6] B. H. Miller and E. D. Dahlberg, Appl. Phys. Lett. **69**, 3932 (1996).
[7] N. J. Gökemeijer, T. Ambrose, and C. L. Chien, Phys. Rev. Lett. **79**, 21 (1997).
[8] N. C. Koon, Phys. Rev. Lett. **78**, 4865 (1997).
[9] V. S. Gornakov, V. I. Nikitenko, L. H. Bennett, H. J. Brown, M. J. Donahue, W. F. Egelhoff, R. D. McMichael, and A. J. Shapiro, J. Appl. Phys. **81**, 5215 (1997).
[10] T. Ambrose and C. L. Chien, J. Appl. Phys. **83**, 6822 (1998).
[11] V. I. Nikitenko, V. S. Gornakov, L. M. Dedukh, Y. P. Kabanov, A. F. Khapikov, A. J. Shapiro, R. D. Shull, A. Chaiken, and R. P. Michel, Phys. Rev. B **57**, R8111 (1998).
[12] S. M. Zhou, K. Liu, and C. L. Chien, Phys. Rev. B **58**, R14717 (1998).
[13] M. D. Stiles and R. D. McMichael, Phys. Rev. B **59**, 3722 (1999).
[14] S. F. Zhang, D. V. Dimitrov, G. C. Hadjipanayis, J. W. Cai, and C. L. Chien, J. Magn. Magn. Mater. **198/199**, 468 (1999).
[15] B. Dieny, V. S. Speriosu, S. S. P. Parkin, B. A. Gurney, D. R. Wilhoit, and D. Mauri, Phys. Rev. B **43**, 1297 (1991).
[16] T. C. Schulthess and W. H. Butler, Phys. Rev. Lett. **81**, 4516 (1998).
[17] J. C. Lodder, *Handbook of Magnetic Materials*, edited by K. H. J. Buschow (Elsevier Science, Amsterdam, 1998), p. 324.
[18] Z. H. Qian, M. T. Kief, P. K. George, J. Sivertsen, and J. H. Judy, J. Appl. Phys. **85**, 5525 (1999).
[19] V. I. Nikitenko, V. S. Gornakov, A. J. Shapiro, R. D. Shull, K. Liu, S. M. Zhou, and C. L. Chien, Phys. Rev. Lett. **84**, 765 (2000).